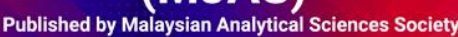
Malaysian Journal of Analytical Sciences (MJAS)





PREPARATION OF CERIUM DOPED NICKEL OXIDE FOR LOWER REDUCTION TEMPERATURE IN CARBON MONOXIDE ATMOSPHERE

(Penyediaan Serium yang Didopkan ke atas Nikel Oksida untuk Suhu Penurunan Lebih Rendah dalam Atmosfera Karbon Monoksida)

Norliza Dzakaria^{1*}, Azizul Hakim Lahuri², Tengku Shafazila Tengku Saharuddin³, Alinda Samsuri⁴, Fairous Salleh⁵, Wan Nor Roslam Wan Isahak⁶, Muhammad Rahimi Yusop⁵, Mohd Ambar Yarmo⁵

¹Advanced Material for Environmental Remediation (AMER) Research Group, Faculty of Applied Science, Universiti Teknologi MARA, Cawangan Negeri Sembilan, Kampus Kuala Pilah, 72000 Kuala Pilah, Negeri Sembilan, Malaysia ²Department of Science and Technology,

Universiti Putra Malaysia Bintulu Campus, 97008 Bintulu, Sarawak, Malaysia

³Faculty of Science and Technology,

Universiti Sains Islam Malaysia, Bandar Baru Nilai, 71800, Nilai, Negeri Sembilan, Malaysia

⁴Department of Chemistry, Centre for Defence Foundation Studies,

Universiti Pertahanan Nasional Malaysia, Kem Sungai Besi, 57000 Kuala Lumpur, Malaysia.

⁵Catalysis Research Group, School of Chemical Sciences and Food Technology, Faculty of Science and Technology

⁶Department of Chemical and Process Engineering, Faculty of Engineering & Built Environment

Universiti Kebangsaan Malaysia, 43600 UKM Bangi, Selangor Darul Ehsan, Malaysia

*Corresponding author: norliza864@uitm.edu.my

Received: 11 May 2021; Accepted: 17 June 2021; Published: 27 June 2021

Abstract

The reduction behavior of cerium nickel oxide (Ce/NiO) catalyst was investigated by using temperature programmed reduction (TPR) with exposure of 40% (v/v) carbon monoxide (CO) in nitrogen atmosphere as a reductant agent. The Ce/NiO catalysts were prepared by using the conventional impregnation method. The reduction characteristics of NiO to Ni were examined up to 700 °C and followed by isothermal reduction. The TPR profiles of doped NiO slightly shifted to a lower temperature from 375 to 366 °C when Ce loading was increased from 3% to 10% (wt./ wt.), respectively. Whereas the undoped NiO was reduced at a higher temperature of 387 °C. XRD diffractogram of the catalysts showed a complete reduction of NiO to Ni. The interaction between cerium and nickel ions for Ce/NiO series leads to a slight decrease in the reduction temperature. Fine sharp particles of Ce deposited on the NiO surfaces were observed through the FESEM images indicating some morphology modification occurred on NiO. It was found that the addition of 10% (w/w) of Ce on NiO also exhibited a larger BET surface area (11.31 $\rm m^2 g^{-1}$) and a smaller average pore diameter (17.7 nm). Based on these results, it is interesting to note that the addition of Ce to NiO has a remarkable influence in reducing the temperature of the reduction process. The 5% Ce/NiO was found sufficient to enhance the reducibility of NiO at a lower temperature.

Keywords: reduction, nickel oxide, cerium, carbon monoxide

Abstrak

Sifat penurunan nikel oksida (NiO) dan serium (Ce) yang didopkan ke atas NiO (Ce/NiO) telah dikaji menggunakan aturcara suhu penurunan (TPR) dengan kehadiran 40% (v/v) karbon monoksida (CO) dalam nitrogen sebagai penurun. Sampel Ce/NiO disediakan menggunakan kaedah impregnasi. Sifat penurunan NiO kepada Ni dikaji dengan peningkatan suhu sehingga 700 °C dan diikuti dengan penurunan isoterma. TPR bagi sampel NiO yang telah didop menunjukkan anjakan isyarat penurunan pada suhu yang lebih rendah daripada 375 °C (3% (bt/bt) Ce/NiO) kepada 365 °C (10% (bt/bt) Ce/NiO). Manakala NiO sahaja diturunkan pada suhu lebih tinggi 387 °C. Difraktogram XRD membuktikan penurunan lengkap bagi NiO kepada Ni. Interaksi di antara ion serium dan nikel bagi siri Ce/NiO menyebabkan suhu penurunan yang lebih rendah. Partikel tajam halus Ce yang terenap pada permukaan NiO diperhatikan melalui imej-imej FESEM menunjukkan terdapat pengubahsuaian morfologinya. Penambahan 10% (bt/bt) Ce pada NiO juga mempamerkan luas permukaan BET yang lebih tinggi (11.31 m²g⁻¹) dan purata diameter liang yang lebih kecil (17.7 nm). Berdasarkan keputusan yang diperolehi, amat menarik untuk menekankan bahawa penambahan Ce ke atas NiO mempunyai pengaruh yang berkesan dalam merendahkan suhu penurunan. Sampel 5% Ce/NiO (bt/bt) didapati mencukupi untuk memperolehi penurunan NiO pada suhu yang lebih rendah.

Kata kunci: penurunan, nikel oksida, serium, karbon monoksida

Introduction

Metal oxides are widely used in technological applications such as coating, catalysis, electrochemistry, optical fibers, and sensors [1, 2]. Nickel oxide (NiO) is an earth-abundant transition metal oxide with superior redox property, electrochemical performance and gas sensing property. Several researchers who studied NiO catalysts with various morphologies for CO oxidation found that ring-like and flower-like NiO demonstrated high activity. Ni is the best catalyst for the reaction by the virtue of its life, high activity and selectivity towards CO oxidation at a lower cost. The partial reduction of nickel oxide under hydrogen at elevated temperature is the most effective method for the preparation of active oxide catalysts [3-6].

Meanwhile, cerium oxide (CeO₂) usually acts as promising materials for chemical transformation mainly for environmental applications and energy conversion systems and sole support or an additive to enhance the catalytic activity of metal oxide catalyst [7-9]. The wide range of properties of CeO₂ such as redox properties, dielectric behavior and thermal stability has seen considerable attention by the researchers [10]. CeO₂ increases the oxygen storage capacity buttresses the metal dispersion of the three ways auto catalysts and enhances CO to CO₂ conversion [11-17]. The presence of transition metal or metal oxides can further enhance their properties. Catalyst performance such as improving the surface area and dispersion of the active

phase was attributed by the presence of transition metal, Ce [18, 19]. The transition metal showed interesting redox properties when cerium is combined with nickel [18]. This material has been widely used for many applications such as a catalyst in automobile engines [20], electrodeposition process [22], water gas shift reaction, CO₂ reforming of methane, water splitting reactions, methane oxidation, hydrogen storage and hydrogen emission [23-26]. The co-deposition of CeO₂ and NiO can improve the corrosion resistance compared to that of pure Ni [27]. A comparison from our previous work showed that NiO as a bimetal catalysts of zirconia doped nickel oxide and cobalt doped nickel oxide gave high reduction temperature in the CO atmosphere as the percentage of zirconia and cobalt increased [28, 29].

The usage of reductant of CO in this work was from the idea of the Boudouard reaction. Instead of using precious H_2 as a reductant, CO can perform the same role in reducing metal oxides. The Boudouard reaction has been known since 1905, it occurs during the gasification of coal and other carbon-rich sources [30]. This reaction is highly endothermic with the equilibrium lies far to the right according to the Le Chatelier's principle. Hence, CO_2 is the favored product (Equation 1).

$$2CO \rightleftharpoons C + CO_2$$
 $\Delta H = -172 \text{ kJ/mol}$ (1)

The free energy of the formation of CO₂ is relatively insensitive to temperature, while the entropy is positive. At high temperatures above 700 °C as typically cited, the free energy change becomes negative, making CO formation progressively more favored. The reaction only plays a significant role in high-temperature (>900 °C) gasification and smelting processes [31, 32]. This reaction has potentially represented a means of CO₂ remediation by converting it to a more synthetically flexible CO. Besides, the reaction has been proposed as part of "clean coal" schemes that convert the CO₂ product gas to CO, which can then be used to produce hydrogen via the water—gas shift reaction or hydrocarbons through the Fischer—Trøpsch process [33].

In this paper, we present a study regarding the reduction behavior of cerium as an additive to nickel oxide at different percentage 3%, 5%, 10% cerium doped (Ce-NiO) and undoped NiO in carbon monoxide by standard wet impregnation method.

Materials and Methods

Catalyst preparation

The NiO (97.0%) and Ce (99.0%) were purchased from Acros Organics Chemical Company and Merck respectively. The ethanol was obtained from ChemAr. The Ce/NiO was prepared by the wet impregnation method. 3 mol % Ce of the total metal cation was dissolved in 5 mL distilled water and 5 mL ethanol. The NiO powder was added corresponding to the metal cation additives in the above proportion. The mixture was stirred vigorously for 2 hours at room temperature. The mixtures were dried at 120 °C overnight and subsequently calcined at 400 °C for 4 hours. The catalysts were denoted as xCe/NiO NiO with x representing the percentage of Ce loading.

Characterization

Temperature programmed reduction (TPR) measurements was performed using a Micromeritic Autochem 2920 Chemisorption Analyzer (Micromeritic, USA). The 50 mg of catalysts were heated up with non-isothermal reduction until 700 °C at 10 °C/ min and followed by isothermal reduction at 700 °C for 60 minutes with 40% CO in N₂ flow at 20 mL/

min (STP) as reducing gas. The carbon monoxide consumption was monitored using a thermal conductivity detector (TCD). Phase characterization was carried out by X-ray diffraction (XRD) Bruker AXS D8 (Bruker, Germany) Advance type with X-ray radiation source of Cu K α (40 kV, 40 mA) to record the 20 diffraction angle from 10-80 degree at the wavelength $\lambda = 0.154$ nm to observe the lattice of the structures. For identification purposes of crystalline phase composition, diffraction patterns obtained were matched with standard diffraction (JCPDS) files.

The N₂ adsorption-desorption isotherms and textural properties were obtained using a static volumetric technique instrument (gas sorption analyzer, Micromeritics ASAP 2020, USA). The Brunauer-Emmett-Teller (BET) surface area was calculated from the isotherms. Approximately 500 mg of catalysts were degassed at 300 °C for 4 hours under vacuum to remove moisture content and humidity gases prior to measurement. The measurement was conducted in a circulating bath of liquid N2 of nitrogen (77 K). The Field Emission Scanning Electron Microscope (FESEM-EDX) technique was used for morphological investigation of the catalysts. A ZEISS MERLIN Compact microscope (MERLIN, Germany) equipped with a field emission gun and EDX probe was employed. The measurements were carried out at an accelerating voltage of 20 kV.

Results and Discussion Temperature programmed reduction

The reduction process of 3%, 5%, 10% (wt./wt.) Ce/NiO and undoped NiO in the CO atmosphere were studied by using CO-TPR as shown in Figure 1. The TPR profile for NiO exhibited a narrower peak compared to Ce/NiO series with one reduction peak ranging from 350 - 400 °C with a maximum peak at 387 °C. The Ce/NiO catalysts exhibited a wider peak due to the addition of Ce on NiO. Nevertheless, the reducing trends were shifted toward lower temperatures. The chemical shift was assumed from the interaction of Ce and Ni particles that led to lower reduction temperature. As the percent of Ce was increased, the reduction temperature was reduced. However, at 10% Ce/NiO was a wider peak among all Ce/NiO series with a maximum reduction

peak at 365 °C. Thus, 5% Ce/NiO was found to be sufficient to reduce the NiO with a maximum reduction temperature of 366 °C. From the result, it was found that the reduction reaction process performed better at a lower percentage of Ce loading. The lower percentage of Ce loading caused Ce particles to be more likely to disperse evenly on the NiO surfaces. Inversely, the Ce particles would be more likely to form larger Ce clusters as the percentage of Ce loading increased. Besides, this might lead to the competition between isolated/fine particle Ce, Ce clusters and NiO to be reduced at the same time. Thus, the reduction temperature did not differ significantly between 10 % and 5 %. For the CeO₂ alone, no reduction peak was observed indicating that there was no reduction process.

Crystallinity analysis using XRD

XRD patterns of calcined 3%, 5%, 10% Ce/NiO and undoped NiO catalysts are shown in Figure 2. All catalysts displayed well-defined diffraction peaks that were matched with NiO peaks with JCPDS file number 03-065-5745. Nonetheless, all peak intensities for

Ce/NiO series were notably lower than NiO. The addition of Ce on NiO affected the nucleation process and then decreased the crystallinity of the catalysts. The increment of Ce loading is believed to affect the intensity of the crystalline peaks of NiO. The highest loading of Ce for 10% Ce/NiO exhibited peaks that were less than half of undoped NiO. Thus, the 10% loading of Ce on NiO led to a decrease in NiO crystallinity. None of Ce peak was observed indicating the Ce particles were well dispersed on the NiO surfaces.

Figure 3 shows XRD patterns of reduced 3% Ce/NiO, 5% Ce/NiO,10% Ce/NiO and undoped NiO catalysts. The complete reduction was observed from NiO to Ni throughout all catalysts. All peaks were matched with Ni with JCPDS file number 01-071-4654. The diffraction peaks were also consistent with the undoped NiO, but it possessed the same trends of the peaks intensity for Ce/NiO series, which were notably lower than NiO catalyst.

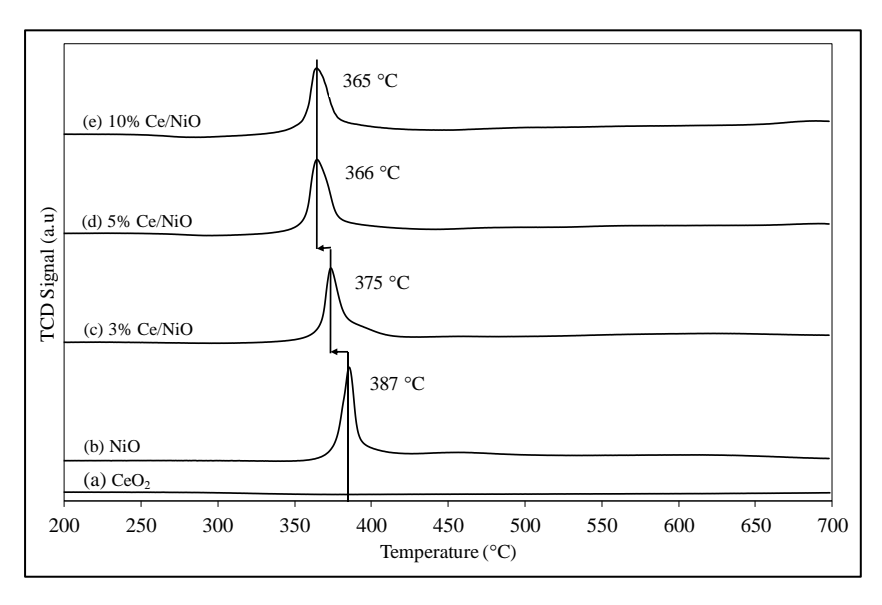


Figure 1. TPR profile of (a) CeO₂, (b) NiO, (c) 3% Ce/NiO, (d) 5% Ce/NiO and (e) 10% Ce/NiO in CO atmosphere

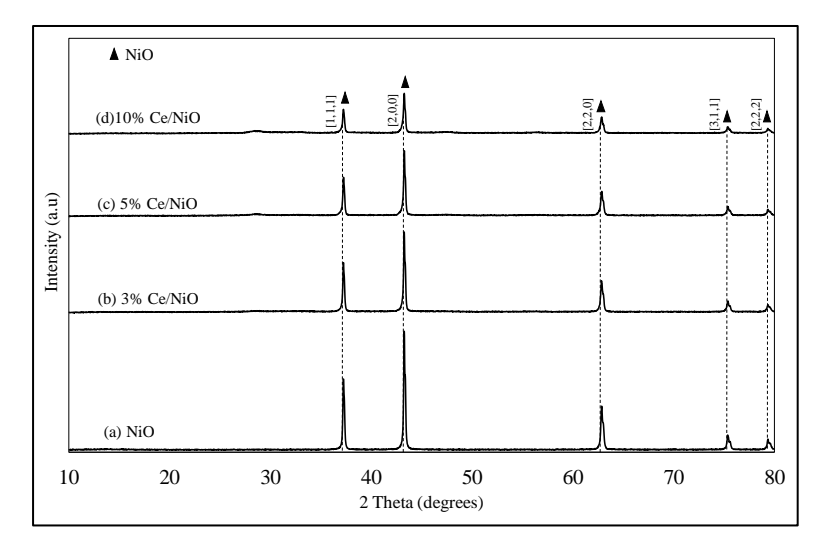


Figure 2. XRD diffractogram of (a) NiO, (b) 3% Ce/NiO, (c) 5% Ce/NiO and (d) 10% Ce/NiO after calcined at 400 °C for 4 hours.

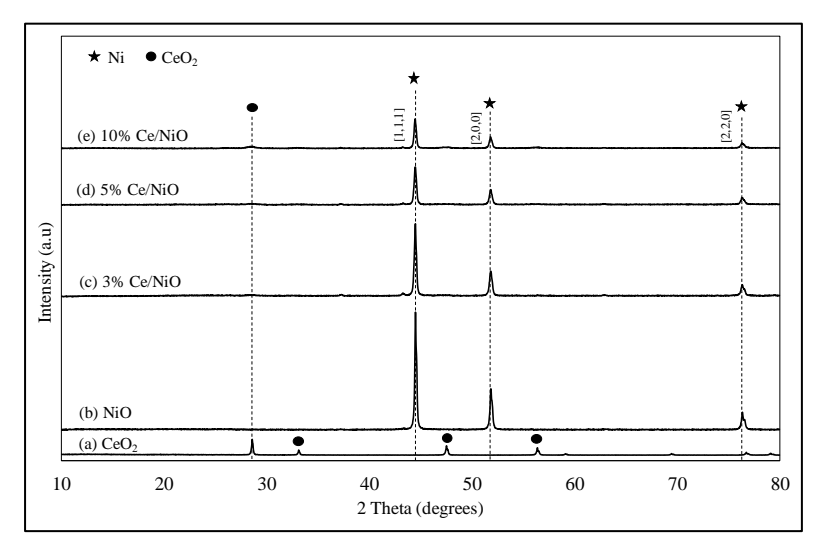


Figure 3. XRD diffractogram (a) NiO, (b) 3% Ce/NiO, (c) 5% Ce/NiO and (d) 10% Ce/NiO after reduction at $700\,^{\circ}\text{C}$

Physical surface analysis

The textural properties of the catalysts were studied through N_2 adsorption-desorption isotherms (Figure 4) and its parameters such as BET surface area, pore volume and average pore diameter (Table 1). The catalysts showed typical isotherms for bimetals catalysts obtained by Lahuri et al. [34,35]. The isotherms are

referring to type III according to IUPAC classification of isotherms, with H3 type hysteresis of desorption branches covering a large range of relative pressure (P/Po) where the adsorbent—adsorbate, interaction is weak but could be obtained with certain porous adsorbents [36]. The hysteresis is proven based on the isotherms ascribed from plate-like particles giving rise

to slit-shaped pores from the adsorbent with large ranges of pore diameters, which does not exhibit any limiting adsorption at high P/Po [37].

The parameters of BET surface area, pore volume and average pore diameter for the catalysts are shown in Table 1. NiO exhibited the smallest specific BET surface area (4.57 m²g⁻¹) and the largest average pore diameter (40.6 nm). The additional percentage of Ce led to the increase of surface area and the decrease of pore diameter. The addition of different percent of Ce reduced the pore diameter [30]. For 10% Ce/NiO, the BET surface area obtained were the highest (11.31 m²g⁻ 1) among all catalysts. It was ascribed to the addition of Ce deposited on NiO surfaces that contributed to the increment of mesopore, which resulted in the reduction of the average pore diameter (17.7 nm). It is believed the modification of Ce/NiO improved the textural properties by increasing the BET surface area, hence, a higher active site could be exposed for any desirable reaction.

Pore size distribution curve of the catalysts is illustrated in Figure 5. Another evidence that Ce loading on NiO contributed to BET surface area significantly was the Ce particles that possessed mesopore structure as shown in the inset of Figure 5. The pore size distribution depended on the distribution of the available pore for each sample. Besides the NiO pore size distribution, the addition of the Ce metal also has its own pore size distribution that alter the overall distribution. Thus, the pore size distribution would change accordingly when the catalyst was loaded with the different percentages of Ce metal loading. It is noteworthy to observe that 3% Ce/NiO exhibited bimodal distribution with high pore size distribution at the region of 450 Å (45 nm) and 810 Å (85 nm). Furthermore, the improvement on the pore size distribution curve for Ce/NiO series catalysts at around 20-50 Å (2 - 5 nm) compared to NiO alone which flattened at this region, is shown in the inset of Figure 5. At above 3% of Ce metal loading, the pore size distribution at the range of 400-1100 Å (40-110 nm) was lower than NiO alone. It was attributed to the agglomeration of Ce metal which reduced available pores.

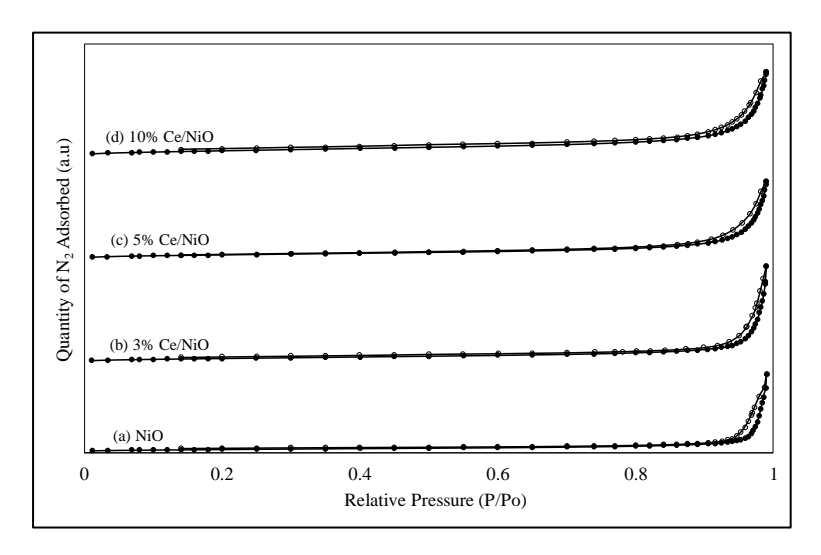


Figure 4. N₂ adsorption-desorption isotherms

Catalyst	S_{BET} (m^2g^{-1})	V _{pore} (cm ³ g ⁻¹)	D _{pore} (nm)
10% Ce/NiO	11.31	0.053	17.7
5% Ce/NiO	8.52	0.049	22.8
3% Ce/NiO	6.82	0.059	32.1
NiO	4.60	0.047	40.6

Table 1. The surface area and pore characterization of the catalysts

^a S_{BET}: BET surface area; V_{pore}: total pore volume; D_{pore}: average pore diameter

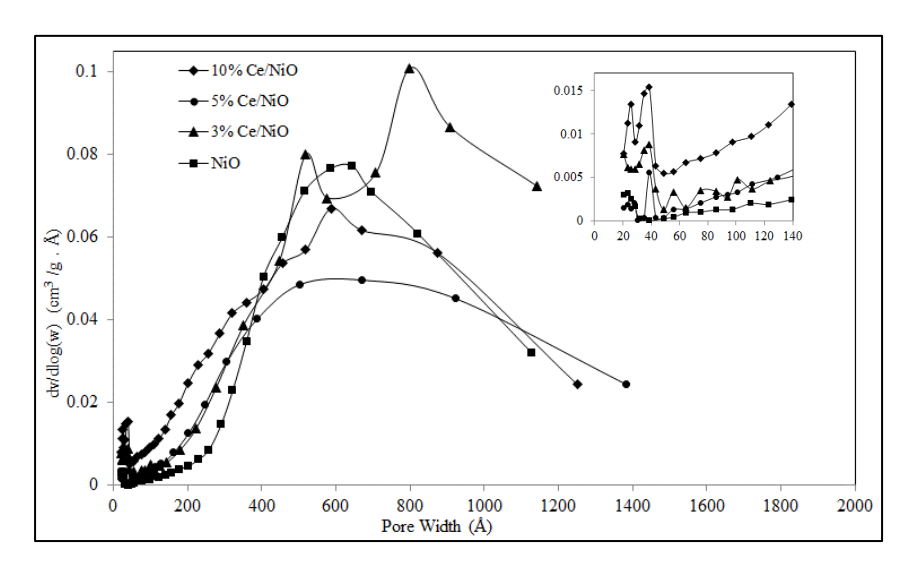


Figure 5. Pore size distribution

Surface morphology by FESEM-EDX

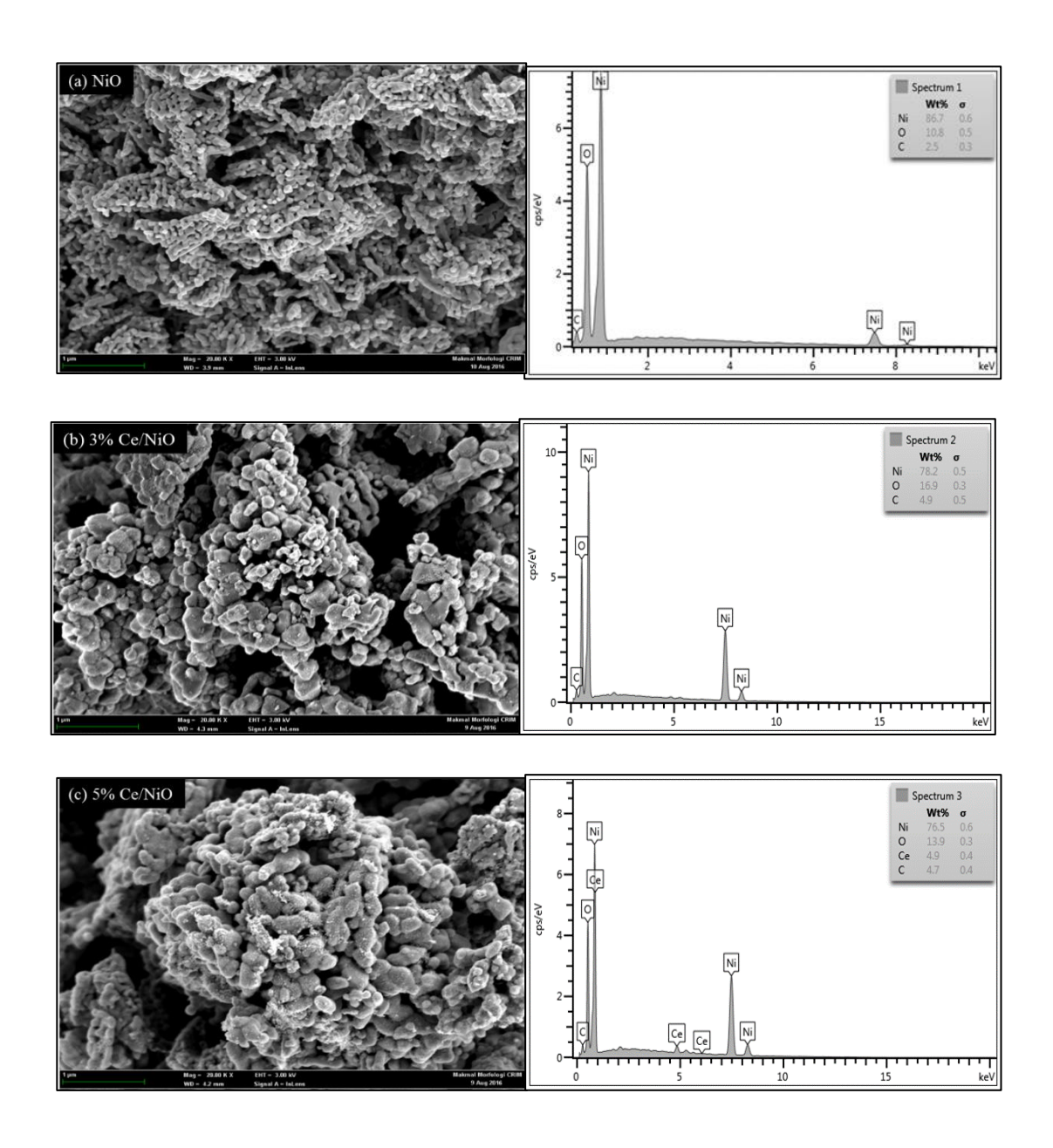
Catalyst morphology was investigated by FESEM and the results are shown in Figure 6. The NiO catalyst showed a rod structure. The addition of Ce to NiO altered the morphology significantly. Besides, the morphologies of NiO catalysts were influenced by Ce. The 3% Ce/NiO exhibited irregular shape and nonuniform particle size distribution of NiO particles with agglomeration forming the bulky size of NiO. For the 5% Ce/NiO catalyst, the NiO was generated in clearer particles. It was believed at 5% Ce addition caused a disturbance in between NiO particles. The 10% Ce/NiO catalyst exhibited more regular spherical particles, smaller particle size and more uniform particle size distribution. The Ce particles deposited on NiO also can be seen with fine sharp particles shape. Hence, these results explain and support the BET surface area results. The NiO catalysts showed different specific surface areas, crystallinity, morphology and surface nickel valence distribution with the different cerium percentages. The experimental temperature, precursor, surfactants and pH control the crystallization of metal oxides with controlled sizes and shapes [31]. Cerium loading on NiO could affect the crystal phase, pore structure and nickel dispersion and then influence oxidative activity [32]. Finally, it could result in a different structure, morphology, surface composition and surface elemental valence for the catalysts. The NiO catalyst showed different structural properties from the Ce/Ni oxide catalysts. The doped metal oxide influenced the structure and morphology of the catalyst [33]. The 10% Ce/NiO catalysts showed regular spherical particles with the highest specific surface area ascribed from the Ce was well dispersed on NiO resulted in

Norliza et al: PREPARATION OF CERIUM DOPED NICKEL OXIDE FOR LOWER REDUCTION TEMPERATURE IN CARBON MONOXIDE ATMOSPHERE

prevention of NiO particles agglomeration. Therefore, the 10% Ce/NiO catalyst showed the highest specific surface area, the lowest crystallinity, the most evenly distributed particle size and the most surface-active Ni²⁺.

The XRD diffractogram did not detect the presence of Ce elements due to the well-dispersed particles on the NiO surface. Nonetheless, according to EDX results, the Ce particles can be detected at 5% loading. The 5% Ce/NiO was the catalysts that contained enough Ce loading to obtain a lower reduction temperature. Hence,

it was proven that the presence of Ce particles could enhance the NiO reduction. The EDX result exhibited a higher weight percentage of Ce for 10% Ce/NiO compared to 5% Ce/NiO due to the EDX was scanned only at a certain targeted area which did not represent the whole sample. It also might be attributed to agglomeration of Ce particles at above 5% of Ce loading which resulted in an uneven distribution of the Ce particles. Nevertheless, this result indicates the presence of Ce on each catalyst.



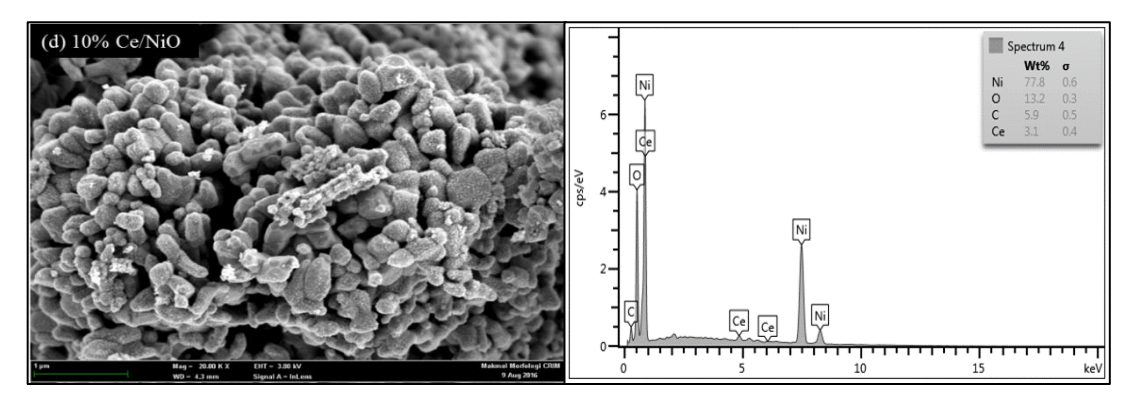


Figure 6. FESEM images and EDX values for (a) NiO, (b) 3% Ce/NiO, (c) 5% Ce/NiO, and (d) 10% Ce/NiO

Conclusion

The reduction behavior of undoped NiO and Ce/NiO catalysts were investigated and compared using the TPR technique and characterized by XRD, BET and FESEM-EDX analysis. The findings in this research revealed that the reduction reaction of NiO obeyed the consecutive mechanism, NiO was reduced to Ni completely. The Ce/NiO also possessed a higher surface area and for FESEM it was clearly shown the Ce was well dispersed on the surface of NiO. Furthermore, the addition of Ce to NiO enhanced a lower reduction temperature. The addition of Ce to the NiO shifted the TPR peaks to the lower temperature. It can be concluded that the reduction temperature of NiO decreases by increasing Ce addition with 5% Ce loading, which is sufficient to reduce NiO to Ni at 366 °C. The Ce changes the coordination environment of nickel and the strength of Ni-O bonds, leading to a decrease in the reduction temperature of doped NiO.

Acknowledgement

The authors wish to thanks Universiti Kebangsaan Malaysia (UKM) for funding this project under research grant number FRGS/1/2015/SG01/UKM/02/2 and GUP-063-2016 from the Ministry of Higher Education (MOHE) Malaysia and Centre of Research and Innovation Management (CRIM) UKM for the instruments facilities.

References

1. Heinrich, V. E. and Cox, P. A. (1994). The surface

- science of metal oxides. Cambridge University Press, Cambridge.
- Pacchioni G. (2000). Ab initio theory of point defects in oxide materials: Structure, properties, chemical reactivity. *Solid State Sciences*, 2: 161-179.
- 3. Maity, A., Ghosh, A. and Majumder, S. B. (2016). Engineered spinel-perovskite composite sensor for selective carbon monoxide gas sensing. *Journal of Sensors and Actuators B: Chemical*, 15: 1-23.
- Moncada, N. G., Navarro, J. C., Odriozola, J. A., Lefferts, L. and Faria, J. A. (2021). Enhanced catalytic activity and stability of nanoshaped Ni/CeO₂ for CO₂ methanation in micro-monoliths. *Catalysis Today*, In Press.
- Dey, S. and Mehta, N. S. (2020). Oxidation of carbon monoxide over various nickel oxide catalysts in different conditions: A review. Chemical Engineering Journal Advances, 1: 100008.
- 6. Janković, B., Adnađević, B. and Mentus, S. (2008). The kinetic study of temperature-programmed reduction of nickel oxide in hydrogen atmosphere. *Chemical Engineering Science*. 63: 567-575.
- Roy, B. and Leclerc, C. A. (2015). Study of preparation method and oxidization/reduction effect on the performance of nickel-cerium oxide catalysts for aqueous-phase reforming of ethanol. *Journal of Power Sources*, 299: 114-124.

- 8. Montini, T., Melchionna, M., Monai, M. and Fornasiero, P. (2016). Fundamentals and catalytic applications of CeO₂-based materials. *Chemical Reviews*, 116: 5987-6041.
- 9. Vita A. (2020). Catalytic applications of CeO₂-based materials. *Catalysts*, 10: 576-580.
- 10. Gangopadhyay, S., Frolov, D., Masunov, A. E. and Seal, S. (2014). Structure and properties of cerium oxides in bulk and nanoparticulate forms. *Journal of Alloys and Compounds*, 584: 199-208.
- 11. Taylor, K. C. (993), Nitric oxide catalysts in automotive systems. *Catalysis Reviews Science Engineering*, 35: 457-481.
- 12. Yao, H. C. and Yao, Y. F. Y. (1984). Ceria in automotive exhaust catalysts: I. Oxygen storage. *Journal of Catalysis*, 86: 254-265.
- 13. Kummer, J. T. (1986). Use of noble metals in automobile exhaust catalysts. *Journal Physical Chemistry*, 90: 4747-4752.
- Oh, S. H. (1990). Effect of cerium addition on the CO-RO reaction kinetics over alumina-supported rhodium catalysts. *Journal of Catalysis*, 124: 477-485.
- 15. Oh, S. H. and Eickel, C. C. (1988). Effects of cerium addition on CO oxidation kinetics over alumina-supported rhodium catalysts. *Journal of Catalysis*. 112: 543-555.
- Loof, P., Kasemo B. and Keck, K. E. (1989).
 Oxygen storage capacity of noble-metal car exhaust catalysts containing nickel and cerium. *Journal of Catalysis*. 118: 339-348.
- 17. Bera, P., Patil, K. C., Jayaram, V., Subbanna, G. N. and Hegde, M. S. (2000). Ionic dispersion of Pt and Pd on CeO₂ by combustion method: Effect of metal–ceria interaction on catalytic activities for NO reduction and CO and hydrocarbon oxidation. *Journal of Catalysis*. 196: 293-301.
- Deraz, N. M. (2012). Effect of NiO content on structural, surface and catalytic characteristics of nano-crystalline NiO/CeO₂ system. *Ceramics International*. 38: 747-753.
- Castano, C. E., O'Keefe, M. J. and Fahrenholtz, W. G. (2015). Cerium-based oxide coatings. *Current Opinion in Solid State & Materials Science*, 19: 69-76.
- 20. Ashif, H. T., Avinash, A. C., Faheem, A. S., Jin, C.

- W. and Kim, H. (2015). Synthesis and application of CeO₂/NiO loaded TiO₂ nanofiber as novel catalyst for hydrogen production from sodium borohydride hydrolysis. *Energy*. 89: 568-575.
- 21. Wang, J., Shen, M., Wang, J., Yang, M., Wang, W., Ma, J. and Jia, L. (2010). Effects of Ni-doping of ceria-based materials on their micro-structures and dynamic oxygen storage and release behaviors. *Catalysis Letter.* 140: 38-48.
- 22. Zeng, Y. B., Qu, N. S. and Hu, X. Y. (2014). Preparation and characterization of electrodeposited Ni-CeO₂ nanocomposite coatings with high current density. *International Journal of Electrochemical Science*, 9: 8145-8155.
- Du, X., Zhang, D., Shi, L., Gao, R. and Zhang, J. (2012). Morphology dependence of catalytic properties of Ni/CeO₂ nanostructures for carbon dioxide reforming of methane. *Journal of Physical Chemistry C*, 116: 10009-10016.
- 24. Lin, X., Zhang, Y., Wang, Z., Wang, R., Zhou, J. and Cen, K. (2014). Hydrogen production by HI decomposition over nickel–ceria–zirconia catalysts via the sulfur–iodine thermochemical watersplitting cycle. *Energy Conversion Management*, 84: 664 670.
- Shao, S., Shi, A., Liu, C. L., Yang, R. Z. and Dong, W. S. (2014). Hydrogen production from steam reforming of glycerol over Ni/CeZrO catalysts. *Fuel Processing Technology*, 125: 1-7.
- Makarshin, L. L., Sadykov, V. A., Andreev, D. V., Gribovskii, A. G., Privezentsev, V. V. and Parmon, V. N. (2015). Syngas production by partial oxidation of methane in a microchannel reactor over a Ni–Pt/La_{0.2}Zr_{0.4}Ce_{0.4}O_x catalyst. *Fuel Processing Technology*, 131: 21-28.
- Hasannejad, H., Shahrab, T. and Jafarian, M. (2012). Synthesis and properties of high corrosion resistant Ni-cerium oxide nano-composite coating. *Material Corrosion*, 63: 9999-10005.
- 28. Dzakaria, N., Abu Tahari, M. N., Saidin, S., Tengku Saharuddin, T. S., Salleh, F., Lahuri, A. H. and Yarmo, M. A. (2020). Effect of cobalt on nickel oxide toward reduction behaviour in hydrogen and carbon monoxide atmosphere. *Material Science Forum*, 1010: 373-378.

- Dzakaria, N., Samsuri, A., Abdul Halim, A., M., Tengku Saharuddin, T. S., Abu Tahari, M. N., Salleh, F., Yusop, M. R., Wan Isahak, W. N. R., Mohamed Hisham, M. W., and Yarmo, M. A. (2020). Chemical reduction behavior of zirconia doped to nickel at different temperature in carbon monoxide atmosphere. *Indonesian Journal of Chemistry*, 20(1): 105-112.
- 30. Bielowicz, B. and Misiak, J. (2020). The impact of coal's petrographic composition on its suitability for the gasification process: The example of polish deposits. *Resources*, 9(9): 111.
- 31. Van Deventer, J. S. J. (1987). The effect of additives on the reduction of chromite by graphite: An isothermal kinetic study. *Thermochim. Acta*, 111: 89.
- 32. Walker Jr, P. L., Rusinko Jr, F. and Austin, L. G. In Advances in Catalysis (1959). Eds.; Academic Press, Volume 11: pp 133.
- 33. Hunt, J. Ferrari, A. Lita, A. Crosswhite, M. Ashley, B. and Stiegman, A. E. (2013). Microwave-specific enhancement of the carbon–carbon dioxide (Boudouard) reaction. *Journal of Physical Chemistry C*, 117 (51): 26871-26880.

- 34. Lahuri, A. H., Yarmo, M. A., Marliza, T. S., Abu Tahari, M. N., Samad, W. Z., Dzakaria, N. and Yusop, M. R. (2016). Carbon dioxide adsorption and desorption study using bimetallic calcium oxide impregnated on iron (III) oxide. *Materials Science Forum*, 888: 479-484.
- 35. Lahuri, A. H., Yarmo, M. A., Abu Tahari, M. N., Marliza, T. S., Tengku Saharuddin, T. S., Mark Lee, W. F. and Dzakaria, N. (2020). Comparative adsorption isotherm for beryllium oxide/iron(III) oxide toward CO₂ adsorption and desorption studies. *Materials Science Forum*, 1010: 361-366.
- 36. Sing, K. S. W., Everett, D. H., Haul, R. A. W., Moscou, L., Pierotti, R. A. and Rouquerol, J. (1985). Reporting physisorption data for gas/solid systems with special reference to the determination of surface area and porosity. *Pure & Applied Chemistry*, 57(4): 603-619.
- 37. Condon, J. B. (2006). Surface area and porosity determinations by physisorption measurements and theory, first edition, Elsevier, Netherland.